PROCEEDINGS B

royalsocietypublishing.org/journal/rspb

Research

Cite this article: Lautenschlager S, Figueirido B, Cashmore DD, Bendel E-M, Stubbs TL. 2020 Morphological convergence obscures functional diversity in sabre-toothed carnivores. *Proc. R. Soc. B* **287**: 20201818. http://dx.doi.org/10.1098/rspb.2020.1818

Received: 28 July 2020
Accepted: 8 September 2020

Subject Category:
Palaeobiology

Subject Areas:
palaeontology, evolution

Keywords:
convergent evolution, functional morphology, computational analysis, *Smilodon*, ecology

Author for correspondence:
Stephan Lautenschlager
e-mail: s.lautenschlager@bham.ac.uk

Electronic supplementary material is available online at https://doi.org/10.6084/m9.figshare.c.5120442.

THE ROYAL SOCIETY PUBLISHING

Morphological convergence obscures functional diversity in sabre-toothed carnivores

Stephan Lautenschlager[1], Borja Figueirido[2], Daniel D. Cashmore[1], Eva-Maria Bendel[3,4] and Thomas L. Stubbs[5]

[1]School of Geography, Earth and Environmental Sciences, University of Birmingham, Edgbaston, Birmingham B15 2TT, UK
[2]Departamento de Ecología y Geología, Facultad de Ciencias, Universidad de Málaga, 29071 Málaga, Spain
[3]Museum für Naturkunde, Leibniz-Institut für Evolutions- und Biodiversitätsforschung, Invalidenstraße 43, 10115 Berlin, Germany
[4]Institut für Biologie, Humboldt-Universität zu Berlin, Invalidenstraße 42, 10115 Berlin, Germany
[5]School of Earth Sciences, University of Bristol, 24 Tyndall Avenue, Bristol BS8 1TQ, UK

SL, 0000-0003-3472-814X; TLS, 0000-0001-7358-1051

The acquisition of elongated, sabre-like canines in multiple vertebrate clades during the last 265 Myr represents a remarkable example for convergent evolution. Due to striking superficial similarities in the cranial skeleton, the same or similar skull and jaw functions have been inferred for sabre-toothed species and interpreted as an adaptation to subdue large-bodied prey. However, although some sabre-tooth lineages have been classified into different ecomorphs (dirk-tooths and scimitar-tooths) the functional diversity within and between groups and the evolutionary paths leading to these specializations are unknown. Here, we use a suite of biomechanical simulations to analyse key functional parameters (mandibular gape angle, bending strength, bite force) to compare the functional performance of different groups and to quantify evolutionary rates across sabre-tooth vertebrates. Our results demonstrate a remarkably high functional diversity between sabre-tooth lineages and that different cranial function and prey killing strategies evolved within clades. Moreover, different biomechanical adaptations in coexisting sabre-tooth species further suggest that this functional diversity was at least partially driven by niche partitioning.

1. Introduction

The sabre-toothed cat *Smilodon fatalis* from the Pleistocene of North America represents one of the most iconic and instantly recognizable vertebrate fossils [1]. Its distinct morphology, characterized by the eponymous elongated canine teeth, has received considerable academic and public attention [2–4]. However, sabre-toothed species were much more diverse and widespread in the fossil record than the prominence of this single well-known species would suggest. Although only loosely defined and not equally distributed across different species, sabre-tooth morphologies, such as elongate and mediolaterally flattened canines, an often anteroposteriorly compressed braincase, and a reduced coronoid process, have evolved several times convergently: in metatherians (thylacosmilines), in eutherians (independently in creodonts, nimravids, barbourofelids and machairodontine felids) and outside of Mammalia in Permian gorgonopsians [5,6] (figure 1).

Through time, sabre-toothed carnivores showed a near-global distribution across North America, Europe, Africa and Asia, and dominated many terrestrial ecosystems during the Permian and the Cenozoic [1,10]. This repeated occurrence of sabre-tooth morphologies in different, often unrelated groups separated by up to 200 Myr has been explained with independent adaptations for subduing large-bodied prey [5,11] (although see [12]). Furthermore, the presence of sabre-tooth

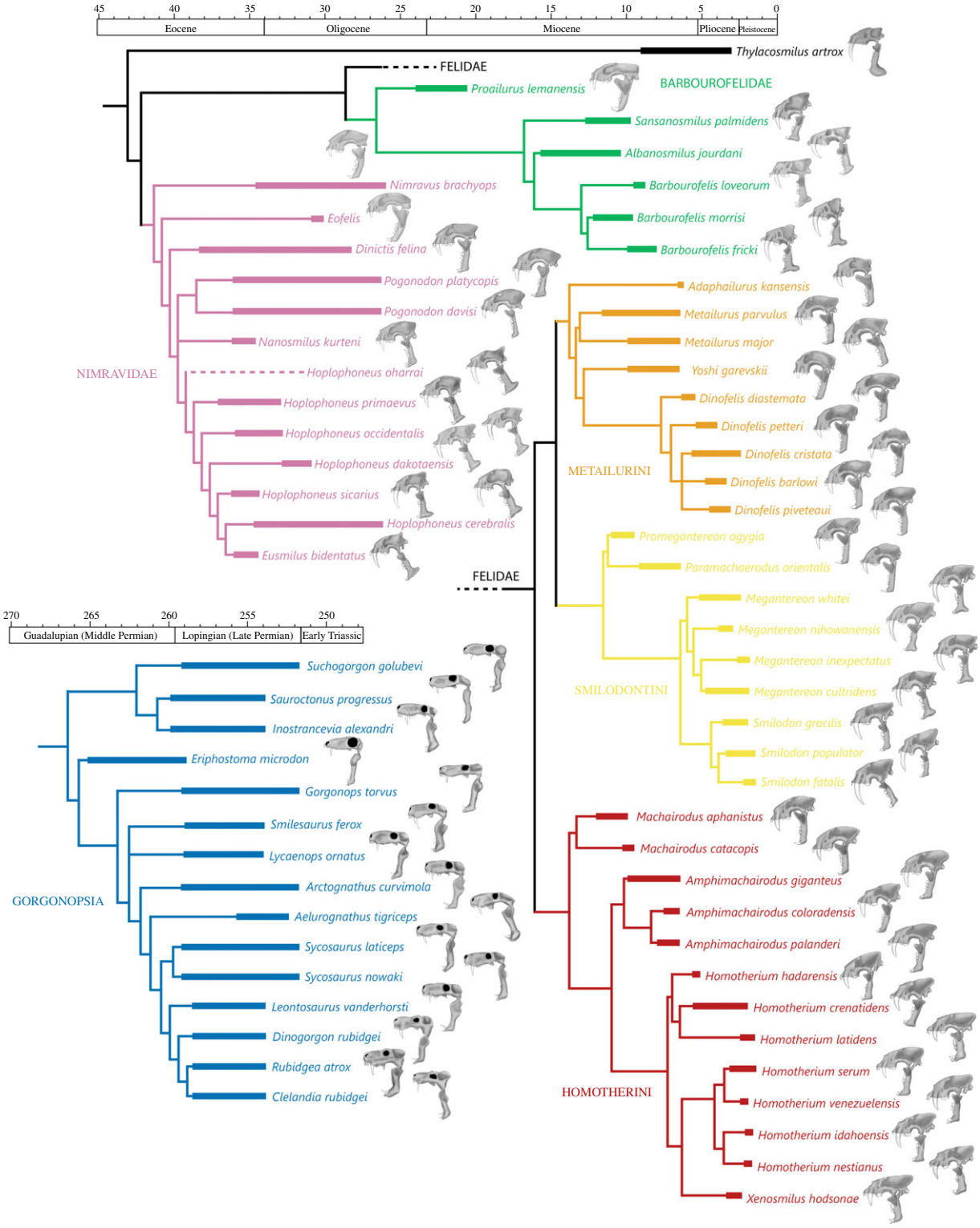

Figure 1. Sabre-toothed vertebrates in their phylogenetic context. Taxa are represented by skull outlines with the mandible opened at the maximum gape angle. Composite phylogenetic tree based on [7–9]. (Online version in colour.)

characters has been hypothesized to provide distinct functional advantages [13], which are thought to represent functional optimization and trend towards increasingly specialized feeding/hunting adaptations in each lineage [14].

Several characters have been discussed as performance indicators in sabre-toothed taxa, including the evolution of a large jaw gape, decreased or increased bite forces and improved stability of the craniodental complex [4,15–17]. However, functional studies of sabre-toothed predators have often focused on single well-known or well-preserved species within each lineage, and these have usually been the most derived taxa impeding inferences about evolutionary trajectories [4,5,16]. This traditional focus on derived taxa has further led to the assumption of functional and evolutionary convergence across sabre-toothed forms. However, caution is warranted over simplified morphological comparisons, as morphological convergence can be a poor indicator for functional convergence [18,19]. Nevertheless, similar ecomorphologies, prey selection, and hunting and killing behaviour have been suggested for all sabre-tooths, although some functional differences between scimitar-toothed and dirk-toothed taxa have been recognized [5,6,17,20,21].

Here, we investigate the evolution of sabre-toothed morphologies across different clades and over the last 265 Myr from a biomechanical perspective. We test the hypothesis that functional trends were decoupled and divergent from morphologically convergent trajectories. Specifically, we obtain biomechanical performance measures (jaw gape, mandibular stability, bite force), which have been demonstrated to correlate with known biologically and ecologically meaningful properties [22–24]. Using a combination of biomechanical modelling and phylogenetic comparative methods, we find that most of the sabre-tooth clades evolved towards different functional specializations acquired via variable evolutionary pathways.

2. Material and methods

(a) Specimen selection

A total of 66 species were sampled from the literature and analysed (figure 1; see electronic supplementary material, figure S1*a*). Only taxa which preserved the complete craniomandibular skeleton were selected, as well as a few incomplete taxa, which could be reconstructed with minimal interpretation. This allowed for over 50% of established species and over 70% of established genera to be sampled in each group. Two-dimensional outlines of each specimen were generated using Adobe Illustrator CC (Adobe Inc.) (electronic supplementary material, figure S1*b*) and muscle attachment sites of the masseter and the temporalis muscle groups were mapped onto the cranial outlines (the pterygoideus group was not considered due to its largely mediolateral line of action and negligible contribution to gape angle and bite force) for the mammalian taxa. For the gorgonopsian taxa, the m. adductor mandibulae externus (m. AME) complex, the pterygoideus muscles and the pseudotemporalis muscles were each considered as a single functional unit.

(b) Gape analysis

For the gape analysis, the images of the cranial outlines were imported into Blender (www.blender.org, v. 2.79) to generate simplified skull and jaw models (electronic supplementary material, figure S1*c*) using a box-modelling approach [25]. The outlines were extruded in the third dimension by a consistent width of 2 mm (we refer to these simplified three-dimensional models as extruded models following [26]).

The gape analysis (figure 2; electronic supplementary material, figure S1*d*) followed the methodology detailed in [27]. The skull and mandible models were joined at the jaw joint and the mandible was allowed full rotation around the mediolateral axis (y-axis) to simulate sagittal opening and closing. Adductor muscles were represented by cylinders connecting the attachment sites projected onto the extruded models. An opening motion with a step size of 0.5° was imposed on the lower jaw, during which the muscle cylinders were stretched. For each step, the ratio between the resting length and the extended length of the muscle cylinders was calculated until any of the muscle cylinders reached the critical extension limit of 170%. This extension limit was based on experimentally derived values for mammalian adductor muscles above which tetanic tension of muscles is no longer possible [27]. Although it cannot be ruled out that the non-mammalian taxa in this study had a different muscle architecture, the same extension limit was assumed for consistency.

To test whether the extruded models could faithfully reproduce realistic results, the methodology was validated using three-dimensional models of fossil sabre-tooths (*Smilodon fatalis*, *Homotherium serum*, *Yoshi garevskii*, *Inostrancevia alexandri*) and extant felids (*Panthera leo*, *Hyena hyena*), which covered the range of observed cranial morphologies (see electronic supplementary material). To further account for uncertainties regarding the exact muscle attachment, five different variations in muscle arrangement were tested for each model and the average gape angle was calculated. To evaluate how much the extruded models underestimate gape angles, a correction factor was calculated (see electronic supplementary material, figures S2–S4). The obtained correction factor of 2.0 was then applied to the results from the extruded models.

(c) Finite-element analysis

To assess the biomechanical performance of the studied taxa, finite-element analyses (FEA) were performed (electronic supplementary material, figure S1*e*). In comparison with full three-dimensional models, the extruded models may not capture the full biological signal. However, it has been demonstrated that meaningful, shape-related biomechanical performance measures can be obtained from extruded models [26,28–31]. Sensitivity tests were performed by comparing FEA results obtained from corresponding extruded and full three-dimensional models for selected taxa (see electronic supplementary material, figures S5 and S6). Only the mandible morphology was considered for FEA, as it can be more accurately replicated in this simplified context. Furthermore, the mandible provides a more reliable signal for feeding performance compared to the skull, which underlies constraints due to compromising functions [24].

For FEA, the extruded models of the lower jaws were exported from Blender as .STL files and imported into HyperMesh (Altair, v. 11) for solid meshing and the setting of boundary conditions. Mesh size was kept uniform to generate a quasi-ideal mesh following [32] (electronic supplementary material, table S1), which allowed the calculation of average stress values. All models were assigned isotropic material properties for bone ($E = 13.7$ GPa, $\upsilon = 0.3$) and teeth ($E = 38.6$ GPa, $\upsilon = 0.4$) [21]. Only the crowns of the canine teeth were considered in each model, representing the functional unit during initial prey contact.

Two functional scenarios were tested. (i) A non-masticatory bending test was performed to investigate mandibular stability under generalized loading conditions [24]. A single ventrally directed nodal force was applied to the tip of the canine tooth. Load forces were scaled following the quasi-homothetic transformation approach of [33], which ensures correct force/surface area scaling for extruded models as used here. Models were further constrained from movement in x-, y- and z-directions at the jaw joint (three nodes). (ii) A second set of analyses were performed with all mandibles scaled to the same size and adductor muscle forces applied. Adductor muscle forces were calculated from the size of the attachment area visible in lateral view multiplied by the specific tension (0.3 N mm^{-2}) [34]. All models were further constrained from movement at the tip of the canine tooth (one node in x- and y-directions, but not z-direction to simulate penetration of the prey by the canine).

All models were imported into Abaqus (Simulia, v. 6.141) for analysis and post-processing. Biomechanical performance was assessed by per element average von Mises stress (with top 1% of magnitudes values excluded to account for artefacts resulting from point loads) and reaction forces measured at the tip of the canine tooth. Tests for statistical significance of the individual performance metrics were performed in PAST 3.22 [35] (electronic supplementary material, tables S2–S4).

(d) Geometric morphometric analysis

To quantify the morphological variation of the analysed taxa, a two-dimensional, landmark-based geometric morphometrics (GMM) approach was used (electronic supplementary material, figure S1*f*). A set of fixed landmarks and semi-landmarks were used to describe the morphology of the skull (8 fixed, 55 semi-landmarks) and the mandible (6 fixed, 25 semi-landmarks; electronic supplementary material, figure S7), digitized with tpsDig2

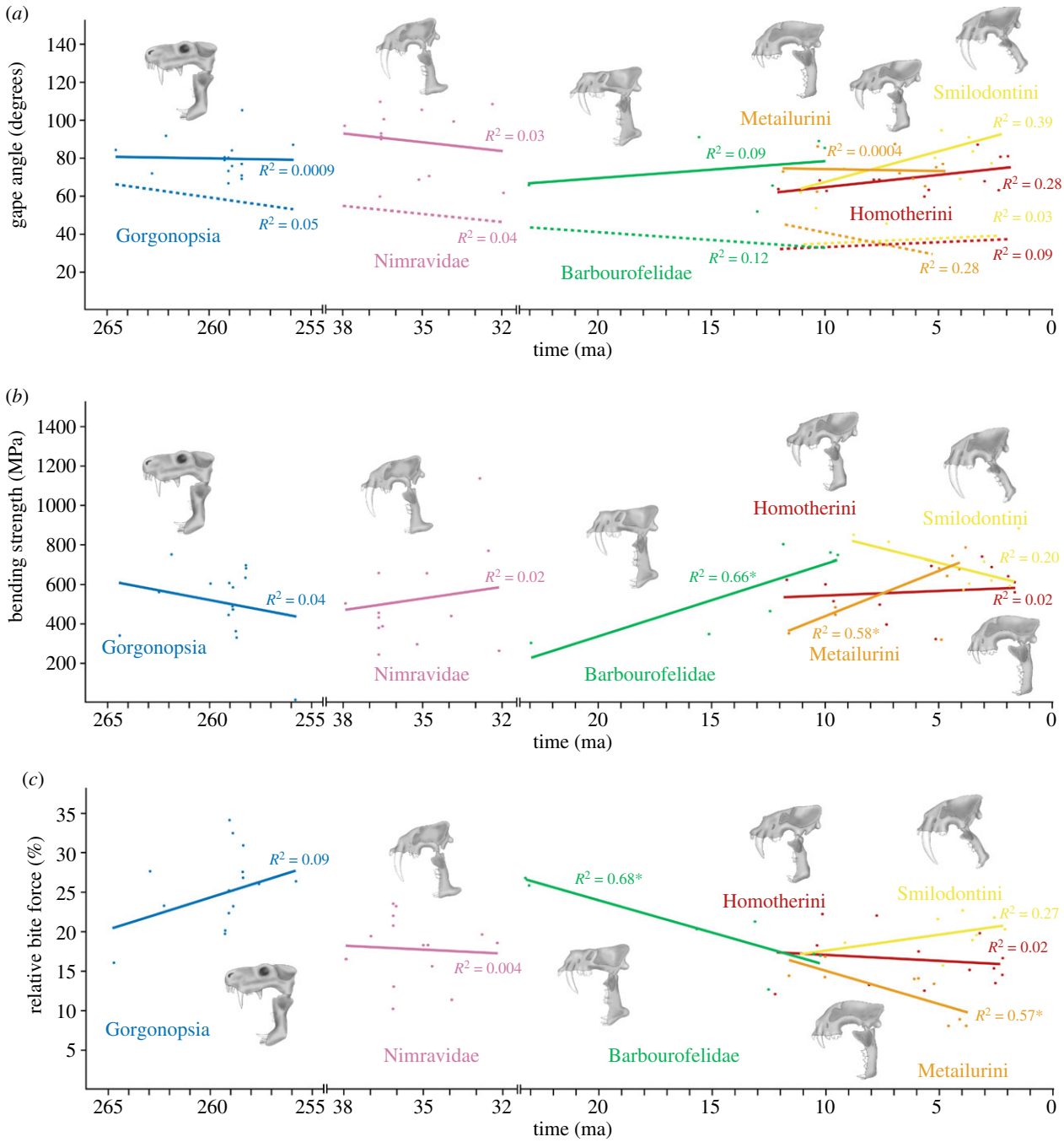

Figure 2. Biomechanical performance for different sabre-toothed clades through time: (*a*) actual (solid lines) and effective (dotted lines) gape angle; (*b*) average bending strength of the mandible tested in non-masticatory scenario; (*c*) relative bite force (bite efficiency) based on ratio between absolute bite forces and muscle forces. (Online version in colour.)

[36]. Landmark coordinates were subsequently superimposed using a procrustes analysis and then subjected to a principal component analysis (PCA) in PAST 3.22 [35]. PCA scores were used to create morphospace plots (electronic supplementary material, figures S8–S10) and to generate performance heatmaps (electronic supplementary material, figure S1*i*) using the R package MBA (https://cran.r-project.org/web/packages/MBA/index.html). Phylomorphospaces were created using the phylogenetic relationships depicted in figure 1.

(e) Phylogeny and evolutionary rates

Time-scaled phylogenetic trees with branch lengths were required to investigate the tempo and mode of biomechanical evolution (electronic supplementary material, figure S1*h*). Tree topologies are composite phylogenies, based on [7,8] for sabre-toothed mammals and [9] for gorgonopsians. The individual sabre-toothed mammal topologies were combined into a single composite tree for the rates analyses. We use the 'equal' [37] and the fossilized birth–death (FBD) [38,39] time-scaling approaches to test for consistency. Temporal data were based on first appearance dates (FADs) and last appearance dates (LADs), representing the bounds of geological intervals that taxa occurred within. Dating uncertainty was incorporated when time-scaling trees by running 100 iterations and, for each iteration, drawing a single occurrence date for each taxon from a uniform distribution between their FAD and LAD. Traitgrams (phenograms) (electronic supplementary material, figure S11) were generated for each biomechanical character for each subgroup using a randomly selected time-calibrated tree for each group, and maximum-likelihood ancestral state estimation in phytools [40].

Rates of biomechanical evolution were analysed using a Bayesian approach with the variable-rates model in BayesTraits v. 2.0.2 [41]. For the 100 time-scaled iterations of the gorgonopsian

tree and the full sabre-toothed mammal tree, rate heterogeneity in each $\log_{10}$ transformed character was tested using a reversible jump Markov chain Monte Carlo algorithm (rjMCMC). Each tree was run for 200 million iterations, parameters were sampled every 16 000 iterations and the first 40 million iterations were discarded as burn-in. The smallest effective sample size (ESS) was used to assess run convergence. To detect shifts in evolutionary rates, the variable-rates model rescales branches where variance of trait evolution differs from that expected in a homogeneous (Brownian motion) model. The resulting 'rate scalars' represent the amount of evolutionary acceleration or deceleration relative to the background rate along each branch [41,42]. Stepping-stone sampling, with 100 stones each run for 1000 iterations, was used to calculate the marginal likelihood of the models (heterogeneous versus homogeneous rates) [43]. Model fit was compared using Bayes factors and the variable-rates post processor was used to extract the final parameter values [42]. We summarized rates results for each character by calculating consensus trees from all time-scaled trees that favoured a heterogeneous rates model—giving the mean rate scalars for each branch across gorgonopsians and sabre-toothed mammal phylogeny. Results were consistent in both the 'equal' (figure 4) and FBD dated trees (electronic supplementary material, figure S12).

3. Results

(a) Maximum jaw gape

The biomechanical analyses demonstrate that gape angles vary considerably between species and groups (figure 2*a*; electronic supplementary material, figure S9*b*). Although there appears to be a trend for the increase (barbourofelids, smilodontines, homotherines) or decrease (nimravids, metailurines) of gape angles through time, none of these relationships are statistically significant (electronic supplementary material, table S2). All species across the different lineages show gape angles between 52° and 111°, but diversification patterns differ considerably between groups. Gorgonopsians and nimravids show an 'early high disparity' pattern and the widest range of gape values, indicating an early and fast diversification. All other groups exhibit a constant to 'late high disparity' trend (electronic supplementary material, figure S12*a*). Effective gape angles (= clearance between upper and lower canines and a proxy for prey size [12]) are considerably lower than the maximum gape angles in all groups (figure 2*a*) but again no statistically significant relationship through time was recovered (electronic supplementary material, table S2). A comparison between actual and effective gape shows a (statistically significant) moderate correlation in homotherines ($R^2 = 0.78$, $p = 6.22 \times 10^{-5}$) and nimravids ($R^2 = 0.65$, $p = 0.0009$) but a more decoupled relationship in the other groups ($R^2 = 0.38$–0.63) (electronic supplementary material, table S2 and figure S13*a*).

The performance heatmap for the gape angle shows an equal complexity in the evolutionary dynamics. Some (but not all) derived taxa in each group occupy regions of higher performance compared to basal forms (for example in gorgonopsians, barbourofelids and smilodontines). However, this is not a uniform trend and exceptions are present in each group (figure 3*b*; electronic supplementary material figures S14*b* and 15*b*), with derived taxa moving towards low-performance regions. For effective gape angles (figure 3*c*), there is movement between areas of similar performance or towards areas of lower performance for the basal taxa in each group (figure 3*c*; electronic supplementary material, figures S14*c* and 15*c*).

Evolutionary rates in jaw gape are heterogeneous for gorgonopsians in the majority of trees analysed (97%). Rapid rates are concentrated in derived rubidgeines, particularly the robustly skulled and large-bodied *Leontosaurus*, *Dinogorgon*, *Rubidgea* and *Clelandina* (figure 4*a*). *Clelandina* evolved the largest gape angle of all gorgonopsians, while *Dinogorgon* and *Leontosaurus* rank among the smallest gapes. Similarly, divergent gape angles in closely related taxa are seen in the *Inostrancevia* (large gape) + *Sauroctonus* (small gape) clade—which also exhibit moderately fast rates. In mammalian sabre-toothed taxa, there is mixed evidence for heterogeneous rates, with only 58% of analytical iterations recovering positive evidence for rate variation (figure 4*b*). In these trees, rapid rates are seen in smilodontines (*Megantereon*, *Smilodon*), derived barbourofelids and nimravids (*Pogonodon*, *Hoplophoneus*, *Eusmilus*).

(b) Bending strength

Bending strength of the mandible was found to significantly increase with time in barbourofelids and metailurines (figure 2*b*; electronic supplementary material, figure S16). While nimravids and homotherines also show an increase in bending strength, this trend is not supported statistically. Similarly, the apparent decrease in gorgonopsians and smilodontines is not statistically significant (figure 2*b*; electronic supplementary material, table S2). Bending strength follows a distinct 'early high disparity' pattern in nimravids and (to a lesser degree) in gorgonopsians and also smilodontines. All other groups show a 'late high disparity' trend (electronic supplementary material, figure S9*b*). Overall, bending strength is not correlated with actual gape ($R^2 < 0.2$) and effective gape ($R^2 < 0.47$) (electronic supplementary material, table S3 and figure S13*b*,*d*).

Similar to gape angle, the evolutionary trends across the performance heatmap show complex movement towards different performance areas (figure 3*d*; electronic supplementary material, figures S14*d* and S15*d*). As recovered above, only in barbourofelids and metailurines there is a clear trend of derived taxa moving towards high-performance areas.

Rates of evolution in bending strength are generally homogeneous for gorgonopsians, with only 20% of iterations showing heterogeneity. By contrast, mammalian sabre-toothed taxa show several bursts of fast evolution in bending strength in 97% of trees. Fast rates are seen in smilodontines and on internal branches uniting metailurines and smilodontines (figure 4*c*). This reflects both great disparity in smilodontines (e.g. *Smilodon populator* versus *Smilodon fatalis*) and the larger difference between generally high bending resistances in smilodontines compared to low bending strengths in basal metailurines (electronic supplementary material, figure S11*b*). Elsewhere, rapid rates are seen in sister taxa that have divergent bending strengths, notably *Homotherium serum* and *Homotherium venezuelensis*, and the nimravids *Eusmilus* and *Hoplophoneus cerebralis* (figure 4*c*).

(c) Bite force

Barbourofelids and metailurines show a statistically significant trend of decreasing bite forces through time. Other groups appear to have a constant (nimravids, homotherines) or increased (gorgonopsians, smilodontines) bite force

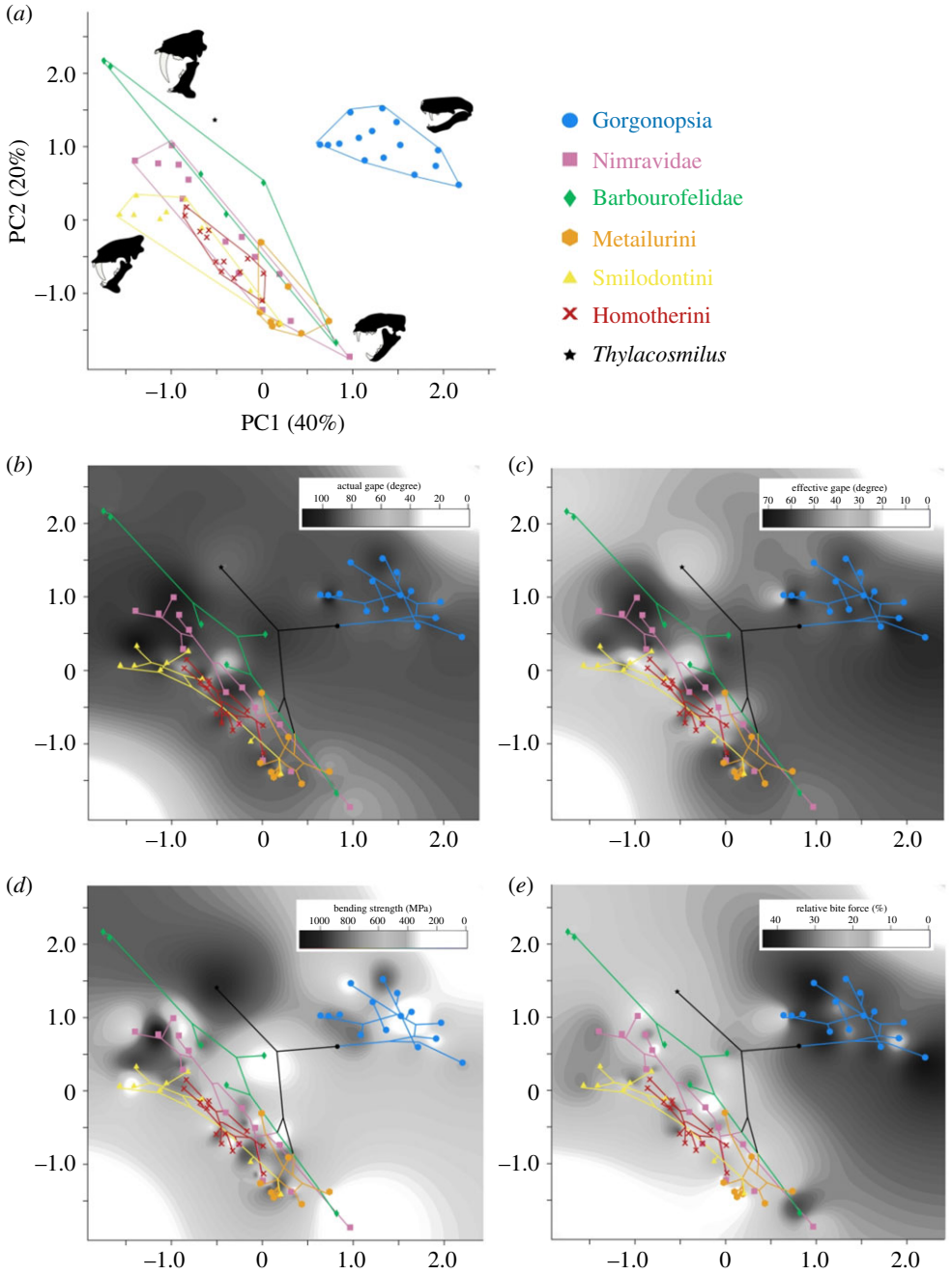

Figure 3. Morphospace and performance space occupation of studied sabre-tooth species (crania and mandibles combined): (*a*) morphospace with convex hulls for different groups obtained from the Procrustes coordinates of the landmark analysis; (*b*) performance heatmap with actual gape angle values plotted onto morphospace; (*c*) performance heatmap with effective gape angle values plotted onto morphospace; (*d*) performance heatmap with bending strength values plotted onto morphospace; (*e*) performance heatmap with bite force values plotted onto morphospace. Phylogenetic relationships as in figure 1 superimposed on heatmaps. (Online version in colour.)

through time, but these trends are not statistically supported (figure 2*c*; electronic supplementary material, figure S17 and table S2). Gorgonopsians explore a wider range of relative bite forces (approx. 15–35%), while the mammalian sabre-tooths are restricted to lower relative bite forces (approx. 10–25%). No or only weak and statistically not significant correlations were found between bite force and actual gape ($R^2 < 0.04$) and bite force and effective gape ($R^2 < 0.3$), whereas a moderate correlation between bending strength and bite force is observed in barbourofelids ($R^2 = 0.77$, $p = 0.03$) and metailurines ($R^2 = 0.54$, $p = 0.026$; electronic supplementary material, table S3 and figure S13*c*,*e*,*f*).

The evolutionary pathways across the performance space show that selected derived taxa in some groups (gorgonopsians, smilodontines) move towards areas of higher performance compared to the basal taxa. However, this trend is not consistent for all derived taxa in these groups. By contrast, barbourofelids and metailurines move towards low-performance areas (figure 3*e*; electronic supplementary material, figures S14e and S15*e*).

In gorgonopsians, again only 11% of iterations show evidence for rate variation, suggesting that a homogeneous rate (Brownian motion) model is favoured. Accelerated rates of bite force evolution were widely distributed in mammalian sabre-toothed taxa (figure 4*d*) and a heterogeneous-rates model is favoured for 94% of analysed trees. Fastest rates are seen in nimravids, particularly *Eusmilus* and *Hoplophoneus*. Other high-rate instances involve taxa that evolved contrasting bite forces compared to their closest relatives. This is seen in homotherines, where *Amphimachairodus* evolved relatively

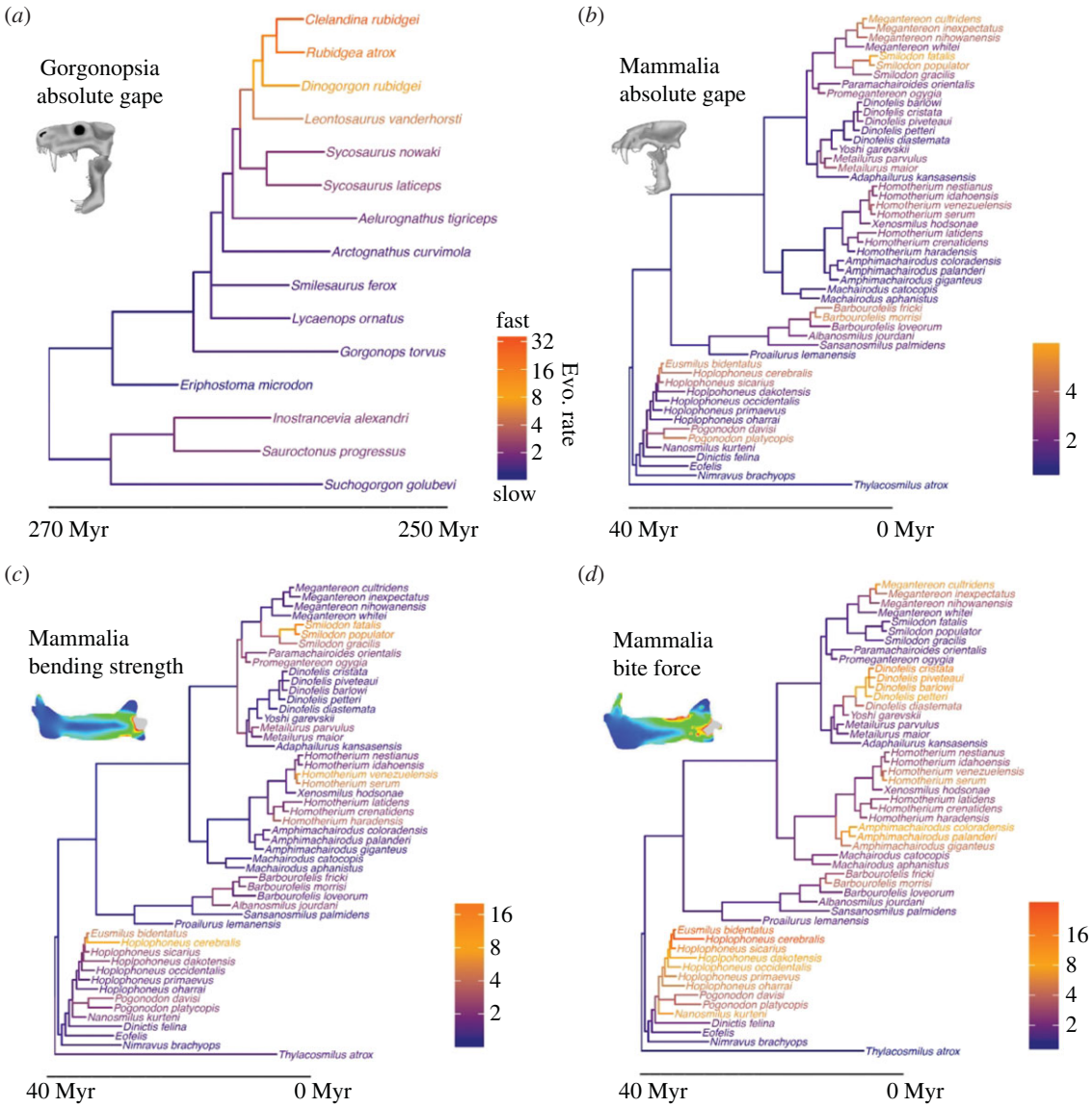

Figure 4. Rates of biomechanical evolution in sabre-toothed vertebrates: (*a*) rates of evolution in gorgonopsian gape angle summarized from 97 heterogeneous rate trees; (*b*) evolutionary rates in sabre-toothed mammal gape angle showing the consensus tree from 58 heterogeneous rate trees; (*c*) rates of evolution in sabre-toothed mammal bending strength summarized from 97 heterogeneous rate trees; (*d*) evolutionary rates in sabre-toothed mammal bite force illustrating consensus results from 94 heterogeneous rate trees. Rates of evolution in gorgonopsian bending strength and bite force were homogeneous. In each plot, phylogenetic branches and tip labels are coloured according to evolutionary rates, grading from slow to fast as denoted by the keys. The branch lengths are scaled to time and based on the average lengths from the time-scaled input trees. Results were consistent in both the 'equal' and FBD dated trees (electronic supplementary material, figure S12). (Online version in colour.)

large bite forces, in metailurines, where *Dinofelis* shows notably smaller bite forces than more basal taxa, and in smilodontines, where *Megantereon* has increased bite force relative to others.

4. Discussion

The acquisition of hypertrophied canine teeth and cranial sabre-tooth characteristics across different vertebrate lineages represents a remarkable example of convergent evolution [14]. Despite the close morphological similarities exhibited by individual groups/species, some more general differentiations have been discussed for derived sabre-tooth felids [44,45]: scimitar-toothed cats (i.e. homotherines) with relatively shorter, broad and coarsely serrated canines, and dirk-toothed cats (i.e. smilodontines) with elongate and finely or unserrated canines, each representing a distinct ecomorphology with different cranial functions, as well as differences in their post-cranial anatomy [46]. Our new analyses demonstrate that morphofunctional differences and evolutionary dynamics of synapsid sabre-tooths are far more complex. Rather than a clear dichotomous split into two ecomorphologies, we observe a spectrum of functional adaptations. Derived from the combination of the analysed functional parameters (actual and effective gape angle, bending strength, bite force), there are no two clades showing the same distribution of parameters and evolutionary rates (figures 2–4; electronic supplementary material, figures S14 and S15). This confirms assumptions from previous studies on tooth morphology, bite depth and post-cranial specializations that sabre-tooth function and prey killing strategies evolved along functionally diverse pathways [12,17,21,47]. Discoveries of mosaic taxa, such as *Xenosmilus hodsonae*, combining scimitar- and dirk-toothed characteristics, had already hinted at the existence of wider morphofunctional diversity [48]. However, it should be noted that only a fraction of the functional trends through

time have been recovered as statistically significant (electronic supplementary material, table S2).

This is likely to be an effect of the divergent functional performances of derived taxa in each group (electronic supplementary material, figure S11) as well as due to the lack of stratigraphic resolution resulting in the same/similar FADs (in particular for gorgonopsians). In all groups, an increase of functional diversity due to the exploration of different functionspace regions (electronic supplementary material, figure S11) can be observed in the derived taxa, which probably dilutes overall trends but lends further proof to the wide diversity of functional adaptations. Consequently, we find no proof for linear functional optimization of groups as a whole.

Generally, the analyses reveal the emergence of individual species and morphologies with high performances through time but with broad functional diversity and widely distributed high rates leading to functional divergence in each group. For example, an adoption of increased jaw gape and mandibular bending strength is found in most groups, as would be expected following the cranial modifications (i.e. rotation of the braincase, reduction of coronoid process, mental process). While actual gape angles show a range of around 60° (reaching up to 111° in *Smilodon fatalis*), effective gape is restricted to a maximum of roughly 70°, with most species ranging between 45° and 65°. This is a similar clearance observed in modern felids [5] and appears to be the most effective gape necessary for prey capture, casting further doubt on the idea of all sabre-tooths being large prey specialists [12]. The significant correlation between actual and effective gape in nearly all groups (electronic supplementary material, table S3) suggests that canine length and jaw gape are equally important factors and that canine penetration is more important than maximizing prey size [12].

Interestingly, within gorgonopsians, the majority of taxa shows actual gape angles below 80° and effective gape angles below 60°, suggesting a possible specialization towards smaller rather than larger prey, possibly as a strategy to conserve energy expenditure [49]. It is therefore possible that the sabre-like canines in gorgonopsians were used to inflict more severe wounds in smaller/similar-sized prey or had an additional function independent of feeding [50,51]. Positioned considerably outside of mammalian synapsids, gorgonopsians were not constrained in their cranial function by a generalized mammalian/carnivoran morphology. In fact, re-modelling of the skull and jaw (e.g. rotation of the facial skeleton, compaction of the braincase, reduction in jaw adductor space, reduction of the coronoid process, increased attachment for post-cranial musculature) is largely absent in gorgonopsians [5]. Furthermore, the gorgonopsian bite technique is significantly dissimilar to that of eutherians: gorgonopsians used a kinetic-inertial jaw-closing system (analogue to modern crocodilians) relying predominantly on the pterygoideus and temporalis muscle groups to deliver powerful and fast jaw closure [6]. However, the taxa included in our analyses do not account for the entire diversity in gorgonopsian morphology but include mostly larger taxa (e.g. Russian species as well as the morphologically advanced Rubidgeinae [52]). Gorgonopsians only show evolutionary bursts in gape evolution within derived rubidgeines, but bite force and bending strength evolved following a homogeneous rates model. This result may, in part, be due to a low sample size for this group and failure to detect rate variation.

While there appears to be a trend towards increased relative bite forces in gorgonopsians and smilodontines, only the decrease of relative bite force through time in barbourofelids and metailurines is statistically supported. This seemingly counterintuitive trend in barbourofelids may be explained by the increasing specialization and evolution of a novel prey killing strategy in derived taxa. With a shift from a killing bite (similar to modern felids) powered by the jaw muscles to a canine-shear bite harnessing the neck musculature [45,47,53], bite force becomes less important. At the same time, the emphasis on large jaw gape and canine clearance requires a reorganization of the jaw adductor musculature, changing the mechanical advantage and therefore constraining the ability to produce high bite forces [4,5,16].

The canine-shear bite has also been accepted as the main killing mode in *Smilodon fatalis* and other smilodontines [3,16]. However, while derived smilodontines have among the highest actual gape angles, bite forces are not decreasing through time as in barbourofelids. This may be because relative bite forces are within a similar range in derived smilodontines (approx. 15–20°) to those in derived barbourofelids (approx. 12–17°). A canine-shear bite is therefore likely to be the main killing style in both groups. However, the lower bending strength of the mandible in derived smilodontines would have, in contrast to barbourofelids with their prominently developed mental processes, required more powerful forelimbs to restrain prey [11,13,47]. Metailurines parallel barbourofelids closely in increasing mandibular bending strength and decreasing relative bite forces through time. However, metailurines do not show the extent of cranial and mandibular modifications indicative of a canine-shear bite. It is therefore possible that these trends reflect an adaptation to small prey in derived metailurines. By contrast, homotherines would have engaged in a different killing technique, as indicated by moderate values and no significant changes through time of all functional parameters. Homotherines probably employed a predatory behaviour between a clamp-and-hold bite (analogue to modern pantherines) and a canine-shear bite as suggested by previous morphological and biomechanical analyses [21,48]. Nimravids generally show high jaw gapes (i.e. majority of taxa with actual gape angles over 90°) and bending strength values with little change through time. This could represent an intermediate killing strategy for nimravids (as previously hypothesized based on the analysis of mandibular force profiles) [13] with a specialization towards large-bodied prey [47] for which large gape angles and bending strength would be necessary.

The evolutionary pathways across the performance heatmaps (figure 3) further support the hypothesis that the different sabre-tooth species and groups pursued different hunting/killing strategies. However, they also show that there is no single consistent trend towards functional optimization as hypothesized in the past [14]. All analysed groups span a wide range between basal and derived members across the heatmaps/morphospace. With the exception of metailurines, which are restricted to small areas of the mandibular, cranial and combined morphospaces, all groups can be found expanding into different regions of the morphospace (figure 3*a*; electronic supplementary material, figures S14*a* and S15*a*). Anatomically, this represents an adoption of 'typical sabre-tooth' morphologies (i.e. anteroposteriorly short but dorsoventrally high skulls, a reduced coronoid process, an expanded mental process) towards one end and the retention of 'cat-like' morphologies (i.e. relatively shorter canines, low

braincase, high coronoid process) at the other end (figure 3*a*; electronic supplementary material, figures S14*a* and S15*a*). Again, gorgonopsians form the exception in occupying mostly distinct areas in the morphospace, with only occasional intrusions into the areas occupied by the mammalian taxa (figure 3*a*; electronic supplementary material, figure S15*a*). This pattern further supports the assumption that felid sabre-tooths were highly specialized but morphofunctionally constrained, possibly due to a high degree of functional integration [8].

It is further noteworthy that metailurines, homotherines and smilodontines show different or even opposing functional performances and that divergent functional morphologies are linked to rapid evolutionary shifts in some derived taxa in each group (figure 4). These three groups had considerable spatial and temporal overlap, with several sabre-tooth species sharing the same ecosystem with each other and other mammalian carnivores [54,55]. Fast rates and different functional performances therefore suggest selective pressures, considerable specialization and niche-partitioning to avoid intra- and interclade competition. Our results parallel previous findings that mandible shape in sabre-toothed cats evolved at a higher rate than in modern conical-toothed cats [7]. This demonstrates that although a large degree of morphological convergence is present in these groups, functional characteristics are much more variable and diverse.

Data accessibility. All data files are available from the Dryad Digital Repository: https://doi.org/10.5061/dryad.6t1g1jwx3 [56].

Authors' contributions. S.L conceived the study and designed the analyses. S.L., D.D.C and T.L.S. conducted the analyses and designed the figures. B.F and E.-M.B. contributed to the datasets. All authors contributed to the writing of the manuscript.

Competing interests. We declare we have no competing interests.

Funding. T.L.S. was funded by ERC grant no. 788203 (INNOVATION). B.F. was funded by the Spanish Ministry of Science and Competitiveness (grant nos CGL2015-68300P and CGL2017-92166-EXP) and Junta de Andalucía (UMA18-FEDERJA-188).

Acknowledgements. The authors are very grateful to Armin Elsler (University of Bristol) for sharing R code that aids the processing and plotting of outputs from BayesTraits. Part of this work was carried out using the computational facilities of the Advanced Computing Research Centre, University of Bristol. Jordi Marcé-Nogue and Robert Brocklehurst are thanked for constructive suggestions improving the manuscript.

References

1. Werdelin L, McDonald HG, Shaw CA. 2018 *Smilodon: the iconic sabretooth*. Baltimore, MD: JHU Press.
2. Warren JC. 1853 Remarks on *Felis Smylodon*. *Proc. Boston Soc. Nat. Hist.* **IV**, 256–258.
3. Akersten WA. 1985 Canine function in *Smilodon* (Mammalia; Felidae; Machairodontinae). *Contrib. Sci. Nat. Hist. Mus. Los Angeles.* **356**, 1–22.
4. McHenry CR, Wroe S, Clausen PD, Moreno K, Cunningham E. 2007 Supermodeled sabrecat, predatory behavior in *Smilodon fatalis* revealed by high-resolution 3D computer simulation. *Proc. Natl Acad. Sci. USA* **104**, 16 010–16 015. (doi:10.1073/pnas.0706086104)
5. Emerson SB, Radinsky LB. 1980 Functional analysis of sabretooth cranial morphology. *Paleobiology* **6**, 295–312. (doi:10.1017/S0094837300006813)
6. Van Valkenburgh B, Jenkins I. 2002 Evolutionary patterns in the history of Permo-Triassic and Cenozoic synapsid predators. *Paleontol. Soc. Pap.* **8**, 267–288. (doi:10.1017/S1089332600001121)
7. Piras P *et al.* 2018 Evolution of the sabretooth mandible: a deadly ecomorphological specialization. *Palaeogeogr. Palaeoclimatol. Palaeoecol.* **496**, 166–174. (doi:10.1016/j.palaeo.2018.01.034)
8. Piras P, Maiorino L, Teresi L, Meloro C, Lucci F, Kotsakis T, Raia P. 2013 Bite of the cats: relationships between functional integration and mechanical performance as revealed by mandible geometry. *Syst. Biol.* **62**, 878–900. (doi:10.1093/sysbio/syt053)
9. Bendel EM, Kammerer CF, Kardjilov N, Fernandez V, Fröbisch J. 2018 Cranial anatomy of the gorgonopsian *Cynariops robustus* based on CT-reconstruction. *PLoS ONE* **13**, e0207367. (doi:10.1371/journal.pone.0207367)
10. Christiansen P. 2013 Phylogeny of the sabretoothed felids (Carnivora: Felidae: Machairodontinae). *Cladistics* **29**, 543–559. (doi:10.1111/cla.12008)
11. Meachen-Samuels JA, Van Valkenburgh B. 2010 Radiographs reveal exceptional forelimb strength in the sabretooth cat, *Smilodon fatalis*. *PLoS ONE* **5**, e11412. (doi:10.1371/journal.pone.0011412)
12. Andersson K, Norman D, Werdelin L. 2011 Sabretoothed carnivores and the killing of large prey. *PLoS ONE* **6**, e24971. (doi:10.1371/journal.pone.0024971)
13. Therrien F. 2005 Feeding behaviour and bite force of sabretoothed predators. *Zool. J. Linnean Soc.* **145**, 393–426. (doi:10.1111/j.1096-3642.2005.00194.x)
14. Van Valkenburgh B. 2007 Déjà vu: the evolution of feeding morphologies in the Carnivora. *Integr. Comp. Biol.* **47**, 147–163. (doi:10.1093/icb/icm016)
15. Antón M, Galobart À. 1999 Neck function and predatory behavior in the scimitar toothed cat *Homotherium latidens* (Owen). *J. Vertebr. Paleontol.* **19**, 771–784. (doi:10.1080/02724634.1999.10011190)
16. Christiansen P. 2007 Comparative bite forces and canine bending strength in feline and sabretooth felids: implications for predatory ecology. *Zool. J. Linnean Soc.* **151**, 423–437. (doi:10.1111/j.1096-3642.2007.00321.x)
17. Slater GJ, Van Valkenburgh B. 2008 Long in the tooth: evolution of sabretooth cat cranial shape. *Paleobiology* **34**, 403–419. (doi:10.1666/07061.1)
18. Losos JB. 2011 Convergence, adaptation, and constraint. *Evolution* **65**, 1827–1840. (doi:10.1111/j.1558-5646.2011.01289.x)
19. Lautenschlager S, Brassey CA, Button DJ, Barrett PM. 2016 Decoupled form and function in disparate herbivorous dinosaur clades. *Sci. Rep.* **6**, 26495. (doi:10.1038/srep26495)
20. Figueirido B, MacLeod N, Krieger J, De Renzi M, Pérez-Claros JA, Palmqvist P. 2011 Constraint and adaptation in the evolution of carnivoran skull shape. *Paleobiology* **37**, 490–518. (doi:10.1666/09062.1)
21. Figueirido B, Lautenschlager S, Pérez-Ramos A, Van Valkenburgh B. 2018 Distinct predatory behaviors in scimitar-and dirk-toothed sabretooth cats. *Curr. Biol.* **28**, 3260–3266. (doi:10.1016/j.cub.2018.08.012)
22. Pierce SE, Angielczyk KD, Rayfield EJ. 2008 Patterns of morphospace occupation and mechanical performance in extant crocodilian skulls: a combined geometric morphometric and finite element modeling approach. *J. Morphol.* **269**, 840–864. (doi:10.1002/jmor.10627)
23. Polly PD, Stayton CT, Dumont ER, Pierce SE, Rayfield EJ, Angielczyk KD. 2016 Combining geometric morphometrics and finite element analysis with evolutionary modeling: towards a synthesis. *J. Vertebr. Paleontol.* **36**, e1111225. (doi:10.1080/02724634.2016.1111225)
24. Tseng ZJ, Flynn JJ. 2018 Structure-function covariation with nonfeeding ecological variables influences evolution of feeding specialization in Carnivora. *Sci. Adv.* **4**, eaao5441. (doi:10.1126/sciadv.aao5441)
25. Rahman IA, Lautenschlager S. 2016 Applications of three-dimensional box modeling to paleontological functional analysis. *Paleontol. Soc. Pap.* **22**, 119–132. (doi:10.1017/scs.2017.11)
26. Morales-García NM, Burgess TD, Hill JJ, Gill PG, Rayfield EJ. 2019 The use of extruded finite-element models as a novel alternative to tomography-based models: a case study using early mammal jaws. *J. R. Soc. Interface* **16**, 20190674. (doi:10.1098/rsif.2019.0674)
27. Lautenschlager S. 2015 Estimating cranial musculoskeletal constraints in theropod dinosaurs. *R. Soc. Open Sci.* **2**, 150495. (doi:10.1098/rsos.150495)

28. Fletcher TM, Janis CM, Rayfield EJ. 2010 Finite element analysis of ungulate jaws: can mode of digestive physiology be determined. *Palaeontol. Electron.* **13**, 1–15.
29. Young MT, Brusatte SL, Ruta M, de Andrade MB. 2010 The evolution of Metriorhynchoidea (Mesoeucrocodylia, Thalattosuchia): an integrated approach using geometric morphometrics, analysis of disparity, and biomechanics. *Zool. J. Linnean Soc.* **158**, 801–859. (doi:10.1111/j.1096-3642.2009.00571.x)
30. Neenan JM, Ruta M, Clack JA, Rayfield EJ. 2014 Feeding biomechanics in Acanthostega and across the fish–tetrapod transition. *Proc. R. Soc. B* **281**, 20132689. (doi:10.1098/rspb.2013.2689)
31. Serrano-Fochs S, De Esteban-Trivigno S, Marcé-Nogué J, Fortuny J, Fariña RA. 2015 Finite element analysis of the cingulata jaw: an ecomorphological approach to armadillo's diets. *PLoS ONE* **10**, e0120653. (doi:10.1371/journal.pone.0120653)
32. Marcé Nogué J, de Esteban-Trivigno S, Escrig Pérez C, Gil Espert L. 2016 Accounting for differences in element size and homogeneity when comparing finite element models: armadillos as a case study. *Palaeontol. Electron.* **19**, 1–22.
33. Marcé-Nogué J, DeMiguel D, Fortuny J, de Esteban-Trivigno S, Gil L. 2013 Quasi-homothetic transformation for comparing the mechanical performance of planar models in biological research. *Palaeontol. Electron.* **16**, 1–15.
34. Thomason JJ, Russell AP, Morgeli M. 1990 Forces of biting, body size, and masticatory muscle tension in the opossum *Didelphis virginiana*. *Can. J. Zool.* **68**, 318–324. (doi:10.1139/z90-047)
35. Hammer Ø, Harper DA, Ryan PD. 2001 PAST: paleontological statistics software package for education and data analysis. *Palaeontol. Electron.* **4**, 1–9.
36. Rohlf FJ. 2010 *Tpsdig 2*. Stony Brook, NY: State University of New York.
37. Brusatte SL, Benton MJ, Ruta M, Lloyd GT. 2008 Superiority, competition, and opportunism in the evolutionary radiation of dinosaurs. *Science* **321**, 1485–1488. (doi:10.1126/science.1161833)
38. Zhang C, Stadler T, Klopfstein S, Heath TA, Ronquist F. 2015 Total-evidence dating under the fossilized birth–death process. *Syst. Biol.* **65**, 228–249. (doi:10.1093/sysbio/syv080)
39. Matzke NJ, Wright A. 2016 Inferring node dates from tip dates in fossil Canidae: the importance of tree priors. *Biol. Lett.* **12**, 20160328. (doi:10.1098/rsbl.2016.0328)
40. Revell LJ. 2012 Phytools: an R package for phylogenetic comparative biology (and other things). *Methods Ecol. Evol.* **3**, 217–223. (doi:10.1111/j.2041-210X.2011.00169.x)
41. Venditti C, Meade A, Pagel M. 2011 Multiple routes to mammalian diversity. *Nature* **479**, 393–396. (doi:10.1038/nature10516)
42. Baker J, Meade A, Pagel M, Venditti C. 2016 Positive phenotypic selection inferred from phylogenies. *Biol. J. Linnean Soc.* **118**, 95–115. (doi:10.1111/bij.12649)
43. Xie W, Lewis PO, Fan Y, Kuo L, Chen MH. 2011 Improving marginal likelihood estimation for Bayesian phylogenetic model selection. *Syst. Biol.* **60**, 150–160. (doi:10.1093/sysbio/syq085)
44. Kurten B. 1968 *Pleistocene mammals of Europe*. London, UK: Routledge Press.
45. Martin LD. 1980 Functional morphology and the evolution of cats. *Trans. Nebraska Acad. Sci.* **8**, 141–154.
46. Anyonge W. 1996 Locomotor behaviour in Plio-Pleistocene sabre-tooth cats: a biomechanical analysis. *J. Zool.* **238**, 395–413. (doi:10.1111/j.1469-7998.1996.tb05402.x)
47. Meachen-Samuels JA. 2012 Morphological convergence of the prey-killing arsenal of sabretooth predators. *Paleobiology* **38**, 1–14. (doi:10.1666/10036.1)
48. Martin LD, Babiarz JP, Naples VL, Hearst J. 2000 Three ways to be a sabre-toothed cat. *Naturwissenschaften* **87**, 41–44. (doi:10.1007/s001140050007)
49. Carbone C, Teacher A, Rowcliffe JM. 2007 The costs of carnivory. *PLoS Biol.* **5**, 1–6. (doi:10.1371/journal.pbio.0050022)
50. Benoit J, Manger PR, Fernandez V, Rubidge BS. 2016 Cranial bosses of *Choerosaurus dejageri* (Therapsida, Therocephalia): earliest evidence of cranial display structures in eutheriodonts. *PLoS ONE* **11**, e22.
51. Kammerer CF. 2016 Systematics of the Rubidgeinae (Therapsida: Gorgonopsia). *PeerJ* **4**, e1608. (doi:10.7717/peerj.1608)
52. Kammerer CF, Masyutin V. 2018 Gorgonopsian therapsids (*Nochnitsa* gen. nov. and *Viatkogorgon*) from the Permian Kotelnich locality of Russia. *PeerJ.* **6**, e4954. (doi:10.7717/peerj.4954)
53. Martin LD, Schultz CB, Schultz MR. 1988 Sabre-toothed cats from the Plio-Pleistocene of *Nebraska. Trans. Nebraska Acad. Sci.* **16**, 153–163.
54. Hunt Jr RM. 1996 Biogeography of the order Carnivora. *Carnivore Behav. Ecol. Evol.* **2**, 485–541.
55. Van Valkenburgh B. 1999 Major patterns in the history of carnivorous mammals. *Annu. Rev. Earth Planet. Sci.* **27**, 463–493. (doi:10.1146/annurev.earth.27.1.463)
56. Lautenschlager S, Figueirido B, Cashmore DD, Bendel E-M, Stubbs TL. 2020 Data from: Morphological convergence obscures functinal diversity in sabre-toothed carnivores. Dryad Digital Repository. (doi:10.5061/dryad.6t1g1jwx3)